

# Mass and Cross-section Measurements of Chargino at Linear Colliders in Large $\tan \beta$ Case

Yukihiro Kato <sup>a,\*</sup>, Keisuke Fujii <sup>b</sup>, Teruki Kamon <sup>c</sup>,  
Vadim Khotilovich <sup>c</sup>, Mihoko M. Nojiri <sup>d</sup>

<sup>a</sup>*Department of Physics, Kinki University, Osaka, Japan*

<sup>b</sup>*High Energy Accelerator Research Organization, Ibaraki, Japan*

<sup>c</sup>*Department of Physics, Texas A&M University, College Station, TX, U.S.A.*

<sup>d</sup>*Yukawa Institute for Theoretical Physics, Kyoto University, Kyoto, Japan*

---

## Abstract

The lighter chargino pair production ( $e^+e^- \rightarrow \tilde{\chi}_1^+ \tilde{\chi}_1^-$ ) is one of the key processes for determination of supersymmetric parameters at a linear collider. If  $\tan \beta$  is a large value, the lighter stau ( $\tilde{\tau}_1^\pm$ ) might be lighter than the  $\tilde{\chi}_1^\pm$ , while the other sleptons stay heavier. This case leads to a cascade decay,  $\tilde{\chi}_1^\pm \rightarrow \tilde{\tau}_1^\pm \nu_\tau$  followed by  $\tilde{\tau}_1^\pm \rightarrow \tilde{\chi}_1^0 \tau^\pm$ , where  $\tilde{\chi}_1^0$  is the lightest supersymmetric particle. This paper addresses to what extent this cascade decay may affect the measurements of the chargino mass and its production cross section.

*Key words:* Supersymmetry, Linear Collider

*PACS:* 11.30.Pb, 13.66.Hk

---



---

\* Corresponding author.

addresses: Department of Physics, Kinki University, 3-4-1 Kowakae, Higashi-Osaka, Osaka, 577-8502, Japan

*Email address:* [katoy@hep.kindai.ac.jp](mailto:katoy@hep.kindai.ac.jp) (Yukihiro Kato).

# 1 Introduction

Supersymmetry (SUSY) is one of the most promising scenarios of physics beyond the Standard Model (SM) and predicts new particles observable at the present or next generation of colliders. It solves the naturalness problem by taming the otherwise quadratically divergent quantum correction to the Higgs boson mass, makes the three gauge forces unify, and opens up a way to ultimate unification of all the fundamental interactions including gravity [1]. If SUSY is the case, we will be able to probe physics at the unification scale by studying its breaking pattern through various measurements of SUSY particles some of which will have been discovered at the Tevatron or the LHC. One of primary goals for an International Linear Collider (ILC) is hence determination of SUSY or SUSY-breaking parameters through precision measurements of masses and couplings of those SUSY particles. The pair production of lighter charginos ( $e^+e^- \rightarrow \tilde{\chi}_1^+ \tilde{\chi}_1^-$ ) is one of the most important processes in this respect since the  $\tilde{\chi}_1^\pm$  is relatively light in most of the parameter space and hence expected to be studied in the early stage of the ILC project. Measurements of its mass and couplings at the ILC have not only been discussed but, for some typical sets of SUSY(-breaking) parameters, also simulated in detail [2].

All of the cases studied in the past, however, assume that the lighter chargino would decay directly into a final state containing the lightest supersymmetric particle (LSP), which is the lightest neutralino ( $\tilde{\chi}_1^0$ ) in most of the SUSY parameter space. At large  $\tan\beta$  values, however,  $\tilde{\tau}_L$ - $\tilde{\tau}_R$  mixing might generate a large mass splitting between  $\tilde{\tau}_1$  and the other sleptons ( $\tilde{\ell} = \tilde{e}, \tilde{\mu}, \tilde{\tau}_2, \tilde{\nu}$ ), yielding a particular mass hierarchy of  $M_{\tilde{\ell}} > M_{\tilde{\chi}_1^\pm} > M_{\tilde{\tau}_1^\pm} > M_{\tilde{\chi}_1^0}$ . If  $\tilde{\chi}_1^\pm$  is gaugino-like, this means that the  $\tilde{\chi}_1^\pm$  will decay at 100% of the times in the cascade mode:  $\tilde{\chi}_1^\pm \rightarrow \tilde{\tau}_1^\pm \nu_\tau$  followed by  $\tilde{\tau}_1^\pm \rightarrow \tilde{\chi}_1^0 \tau^\pm$ . Consequently, the experimental signature of the chargino pair production will be an acoplanar  $\tau$  pair with significant missing energy carried away not only by the LSP's from the  $\tilde{\tau}_1^\pm$  decays but also by the final-state neutrinos from the  $\tilde{\chi}_1^\pm$  and  $\tau$  decays. This would make it significantly more difficult to determine the chargino mass.

This paper describes results from our simulation studies of the pair production of the lighter charginos and their subsequent cascade decays:  $e^+e^- \rightarrow \tilde{\chi}_1^+ \tilde{\chi}_1^- \rightarrow \tilde{\tau}_1^+ \nu_\tau + \tilde{\tau}_1^- \bar{\nu}_\tau$  in a particular scenario of the Minimal Supersymmetric Standard Model (MSSM), where  $M_{\tilde{\tau}_1^\pm} = 152.7 \text{ GeV}/c^2$  and  $M_{\tilde{\chi}_1^0} = 86.4 \text{ GeV}/c^2$  as in Refs. [3, 4]. It should be noted that signals from the  $\tilde{\tau}^\pm$ - $\tilde{\chi}_1^\pm$  co-annihilation region are recently of great interest. The region is characterized by a difference in the  $\tilde{\tau}^\pm$  mass and the lightest neutralino mass of about 5-15  $\text{GeV}/c^2$ . This small mass difference allows the  $\tilde{\tau}^\pm$  to co-annihilate in the early universe along with the neutralinos in order to produce the current amount of cold dark matter density of the universe measured by WMAP [5]. However, the experimental signature is very challenging. We will not address this signature,

because it requires to detect electron/positron from two-photon process in the forward region. Thus it requires a different optimization of the event selection criteria [6, 7, 8].

## 2 Monte Carlo Simulation

In simulating the signal and various background events, we use the HELAS library [9] to calculate the helicity amplitudes, the BASES/SPRING package [10] to generate the final-state partons, and TAUOLA [11] to decay the final-state  $\tau$  leptons if any, so as to take into account possible spin correlations of intermediate heavy partons, effects of beamstrahlung and subsequent beam-energy spread [12], and finite  $\tau$  polarizations. The generated events are then processed through a fast simulator of a detector model [13], which includes a central tracker, electromagnetic and hadron calorimeters, and muon drift chambers. This simulator smears charged-track parameters in the central tracker with parameter correlation properly taken into account, and simulates calorimeter signals as from individual segments. Although  $\tau$  polarization varies in general with the SUSY parameters and would thus influence the property of the final states, we fix the  $\tau$  polarization for the signal process at the nominal value of 0.026 for simplicity.

For SUSY events, we choose our reference SUSY point to have  $\tan\beta = 50$ ,  $\mu = 400$  GeV,  $m_0 = 200$  GeV, and  $M_2 = 180.0$  GeV, where  $\mu$ ,  $m_0$ , and  $M_2$  are the higgsino mixing mass, universal scalar mass at GUT scale, and  $SU(2)_L$  gaugino mass parameters, respectively. We take  $M_1$  so that it satisfies GUT relation  $M_1 \cong 0.5M_2$ . It corresponds to  $M_{\tilde{\chi}_1^\pm} = 171.0$  GeV/ $c^2$  ( $M_{\tilde{\chi}_1^\pm}^{\text{ref}}$ ),  $M_{\tilde{\chi}_1^0} = 86.4$  GeV/ $c^2$ , and  $M_{\tilde{\tau}_1^\pm} = 152.7$  GeV/ $c^2$ . Notice that  $\tilde{\tau}_1^\pm$  is the next to the lightest SUSY particle (NLSP) and decays to  $\tilde{\chi}_1^0\tau$  at 100% of the time. We assume in what follows that  $M_{\tilde{\chi}_1^0}$  and  $M_{\tilde{\tau}_1^\pm}$  will have been measured below the threshold of chargino pair production, say at  $\sqrt{s} = 310$  GeV, with uncertainties expected for  $\int \mathcal{L}dt = 100$  fb $^{-1}$  [4]. In order to evaluate to what extent we can determine the chargino mass in this setting, we then vary the  $\tilde{\chi}_1^\pm$  mass around 171.0 GeV/ $c^2$ , while keeping the  $\tilde{\tau}_1^\pm$  and  $\tilde{\chi}_1^0$  masses unchanged, by appropriately adjusting the values of SUSY(-breaking) parameters<sup>1</sup> and see how the observable distributions respond to the change.

As for the ILC parameters, we assume  $\sqrt{s} = 400$  GeV,  $\int \mathcal{L}dt = 200$  fb $^{-1}$ , and an electron beam polarization of  $\mathcal{P}(e^-) = -0.9$  (left handed). The  $\tilde{\chi}_1^+\tilde{\chi}_1^-$  production cross section at  $\mathcal{P}(e^-) = -0.9$  is 20 times larger than that at

---

<sup>1</sup> For this we allow violation of the GUT relation between the  $U(1)$  and  $SU(2)_L$  gaugino mass parameters ( $M_1$  and  $M_2$ ) that has been assumed for our reference point.

$\mathcal{P}(e^-) = +0.9$  (right handed). Furthermore, it can suppress the cross section for the  $e^+e^- \rightarrow \tilde{\tau}_1^+ \tilde{\tau}_1^-$  process that yields almost the same final states as our signal process.

### 3 Event Selection

In our setting, the chargino pair production results in a final state consisting of a  $\tau$ -pair with large missing energy. The five major backgrounds for the signal event are considered: (i)  $\tilde{\tau}_1^\pm$ -pair production:  $\tilde{\tau}_1^+ \tilde{\tau}_1^- \rightarrow \tau^+ \tilde{\chi}_1^0 + \tau^- \tilde{\chi}_1^0$ , (ii) neutralino pair production:  $\tilde{\chi}_1^0 \tilde{\chi}_2^0 \rightarrow \tilde{\chi}_1^0 + \tilde{\tau}_1 \tau \rightarrow 2\tilde{\chi}_1^0 + \tau^+ \tau^-$ , (iii) diboson production:  $W^+ W^- \rightarrow \tau^+ \nu_\tau + \tau^- \bar{\nu}_\tau$ ,  $Z^0 Z^0 \rightarrow \tau^+ \tau^- + \ell^+ \ell^-$  ( $\ell = e, \mu, \tau$ ) or  $\tau^+ \tau^- + \bar{\nu} \nu$ , (iv) single boson production:  $eeZ^0$  and  $\nu\nu Z^0$  with  $Z^0 \rightarrow \ell^+ \ell^-$  or  $\nu\bar{\nu}$ , and (v) two-photon  $\tau$ -pair production:  $e^+e^- \rightarrow e^+e^- \tau^+ \tau^-$ . As for the neutralino pair production, the  $SU(2)_L$  relation between  $\tilde{\chi}_2^0$  and  $\tilde{\chi}_1^\pm$  masses is assumed. We also assume the  $\tilde{\chi}_2^0$  mass is measured via other processes such as  $\tilde{\chi}_2^0 \tilde{\chi}_2^0 \rightarrow 4\tau + 2\tilde{\chi}_1^0$ . We ignore the uncertainty in the  $\tilde{\chi}_2^0$  mass measurement, because the effect in  $\tilde{\chi}_1^\pm$  mass measurement is found to be negligible.<sup>2</sup> Notice that the cross section times branching fraction for  $W$ -pair production followed by  $W \rightarrow \ell\nu$  decays is, for instance, eight times higher than that of the signal at our SUSY reference point. We had thus better avoid events with purely leptonic  $\tau$  decays. Notice also that the two  $\tau$ -jets<sup>3</sup> in the SUSY events are likely to be more acoplanar than those from the SM backgrounds. These observations lead us to the following selection criteria to improve signal-to-background ratio:

- (a) there should be no  $e/\mu$  candidates positively identified in the detector simulator;
- (b) jet clustering has to yield two jets with  $5 \text{ GeV} \leq E_{\text{jet}} \leq 160 \text{ GeV}$  for  $y_{\text{cut}} \geq 0.0025$  [14];
- (c)  $-Q_i \cdot J_{iz}/|\vec{J}_i| \leq 0.8$ , where  $Q_i$  and  $\vec{J}_i$  are the charge and the momentum of  $i$ -th jet with  $i = 1(2)$  corresponding to the higher (lower) energy jet;
- (d)  $M_{\text{jet}} \leq 3 \text{ GeV}/c^2$ ;
- (e) the missing transverse momentum  $P_T^{\text{miss}} \geq 20 \text{ GeV}/c$ ;
- (f)  $\cos\theta(J_1, P_{\text{vis}}) \leq 0.9$  or  $\cos\theta(J_2, P_{\text{vis}}) \geq -0.7$ , where  $\cos\theta(J_i, P_{\text{vis}}) \equiv \vec{J}_i \cdot \vec{P}_{\text{vis}}/(|\vec{J}_i||\vec{P}_{\text{vis}}|)$  and  $\vec{P}_{\text{vis}}$  is the visible momentum vector calculated with both tracker and calorimeter information;
- (g) thrust  $\leq 0.98$ ;
- (h) acoplanarity angle  $\theta_A \geq 30^\circ$ .

<sup>2</sup> The  $\tilde{\chi}_1^\pm$  mass determination accuracy is estimated to be  $\pm 0.02 \text{ GeV}/c^2$  if the  $\tilde{\chi}_2^0$  mass fluctuation is  $\pm 1 \text{ GeV}/c^2$ .

<sup>3</sup> A group of particles coming from a  $\tau$  decay will hereafter be called a  $\tau$ -jet even if it contains only one charged particle.

Cut (f) effectively rejects the  $WW$  background, because the  $\tau$  lepton from  $W \rightarrow \tau\nu$  tends to go in the parent  $W$ -boson momentum direction.

We tabulate the resultant selection efficiencies after each cut for the signal and the background processes at the reference SUSY point in Table 1. Total selection efficiency ( $\epsilon_{\text{tot}}$ ) for the  $\tilde{\chi}_1^+ \tilde{\chi}_1^-$  signal at the reference point is  $\epsilon_{\text{tot}}^{\text{ref}} = (15.8 \pm 0.1)\%$ . We see that the selection criteria are effective at suppressing the SM backgrounds, yielding a signal-to-background ratio of 1.7. As for the  $ZZ \rightarrow \nu\nu q\bar{q}$  event where quark jets are mis-identified as  $\tau$ -jets, the total selection efficiency is small (less than  $5.0 \times 10^{-5}$ ) and the expected number of the  $ZZ \rightarrow \nu\nu q\bar{q}$  events is 2.5. We do not include this process in Table 1. We also show the signal selection efficiencies for different chargino masses in Table 2. The  $\tilde{\tau}_1^\pm$  and  $\tilde{\chi}_1^0$  masses are fixed to be  $152.7 \text{ GeV}/c^2$  and  $86.4 \text{ GeV}/c^2$ , respectively. The statistical uncertainty in the efficiency for each point is better than 0.1%. The efficiency depends on the  $\tilde{\chi}_1^\pm$  mass only very weakly as long as  $\Delta M \equiv M_{\tilde{\chi}_1^\pm} - M_{\tilde{\tau}_1^\pm}$  is large enough to deposit a jet energy of  $E_{\text{jet}} \gtrsim 5 \text{ GeV}$  in the detector.

## 4 Results

### 4.1 Determination of chargino mass

If  $\tilde{\chi}_1^0$  and  $\tilde{\tau}_1^\pm$  masses are predetermined, the  $\tau$ -jet energy distribution can be used to determine the  $\tilde{\chi}_1^\pm$  mass, since the shape of the distribution, especially around the endpoint, depends on  $\Delta M$ . As  $\Delta M$  increases, the peak of the distribution shifts to the higher energy side, while the endpoint moves to the lower energy side. This can be seen in Figure 1, which plots the  $\tau$ -jet energy distributions for various  $\Delta M$  values.

In order to determine the chargino mass using the  $\tau$ -jet energy distribution, we first prepare a parametrized  $\tau$ -jet energy distribution (a template) as a function of  $M_{\tilde{\chi}_1^\pm}$  in the following manner: (i) the  $\tau$ -jet energy distribution, including the backgrounds, is fit to a polynomial function by MINUIT [15] for each of high statistics samples with different  $\tilde{\chi}_1^\pm$  masses; (ii) the fitting parameters are then parametrized as a function of  $M_{\tilde{\chi}_1^\pm}$ . Although the  $\tau$ -jet energy distribution may depend on the remaining free parameters such as  $\tilde{\nu}$  mass,  $\mu$  parameter, and  $\tau$  polarization, those are fixed in the present study.

We then compare the  $\tau$ -jet energy distribution for a Monte Carlo sample corresponding to  $200 \text{ fb}^{-1}$  with the template and calculate  $\chi^2$ . Figure 2 shows  $\Delta\chi^2 \equiv \chi^2 - \chi_{\text{min}}^2$  for the reference point ( $M_{\tilde{\chi}_1^\pm}^{\text{ref}} = 171.0 \text{ GeV}/c^2$ ). The fitted value of the  $\tilde{\chi}_1^\pm$  mass is  $170.5 \pm 0.6 \text{ GeV}/c^2$ . This is about  $1\sigma$  off the reference

Table 1. Cumulative selection efficiencies ( $\epsilon$ ) for signal ( $\tilde{\chi}_1^+ \tilde{\chi}_1^-$ ) and various sources of backgrounds. The cross section includes branching ratios of  $W \rightarrow e\nu, \mu\nu, \tau\nu$  for  $W^+W^-$  process and  $Z^0 \rightarrow ee, \mu\mu, \tau\tau, \nu\nu$  for  $Z^0Z^0$ ,  $eeZ^0$ , and  $\nu\nu Z^0$  processes.

[illegible]

Table 2

Total selection efficiencies for five different chargino masses where  $M_{\tilde{\tau}_1^\pm} = 152.7$   $\text{GeV}/c^2$  and  $M_{\tilde{\chi}_1^0} = 86.4$   $\text{GeV}/c^2$ .

$M_{\tilde{\chi}_1^\pm}$ ( $\text{GeV}/c^2$ )	161.0	166.0	171.0	176.0	181.0
	(ref.)				
$\Delta M(\equiv M_{\tilde{\chi}_1^\pm} - M_{\tilde{\tau}_1^\pm})$ ( $\text{GeV}/c^2$ )	8.3	13.3	18.3	23.3	28.3
$\sigma$ (fb)	433	378	322	268	214
$\epsilon_{\text{tot}}$	0.156	0.157	0.158	0.158	0.158
$\mu = 400$ GeV, $\tan\beta = 50$ , $\tau$ polarization = 0.026, $\mathcal{P}(e^-) = -0.9$					

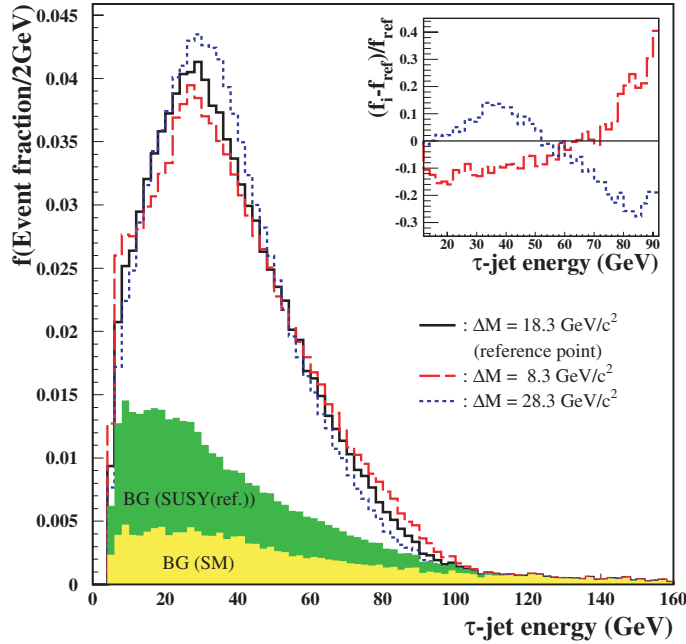


Fig. 1. Energy distributions of  $\tau$ -jets in the signal + background events for 3 representative choices of  $\Delta M$  after our final selection criteria (Table 1). We also show background events. The shape in the reference SUSY scenario ( $\Delta M = 18.3$   $\text{GeV}/c^2$ ) is compared to other cases ( $\Delta M = 8.3$  and  $28.3$   $\text{GeV}/c^2$ ).

mass of  $171.0$   $\text{GeV}/c^2$ . We prepare approximately 100 statistically independent samples of  $\tilde{\chi}_1^\pm \tilde{\chi}_1^\pm$  and  $\tilde{\chi}_2^0 \tilde{\chi}_1^0$  events for the reference point. Each sample is also corresponding to  $200 \text{ fb}^{-1}$ . The  $\chi^2$  fitting procedure provides consistently a  $1\sigma$  uncertainty of  $\pm 0.6$   $\text{GeV}/c^2$  for each sample. However the fluctuation of  $\tilde{\chi}_1^\pm$  mass at the  $\chi^2_{\text{min}}$  is  $\pm 0.4$   $\text{GeV}/c^2$  around the  $M_{\tilde{\chi}_1^\pm}^{\text{ref}}$ . Therefore, we assign the total uncertainty in the  $\tilde{\chi}_1^\pm$  mass measurement to be  $\pm 0.7$   $\text{GeV}/c^2$  (quadratic sum of two sources).

The above estimate ignores the uncertainties in the input  $\tilde{\tau}_1^\pm$  and  $\tilde{\chi}_1^0$  masses.

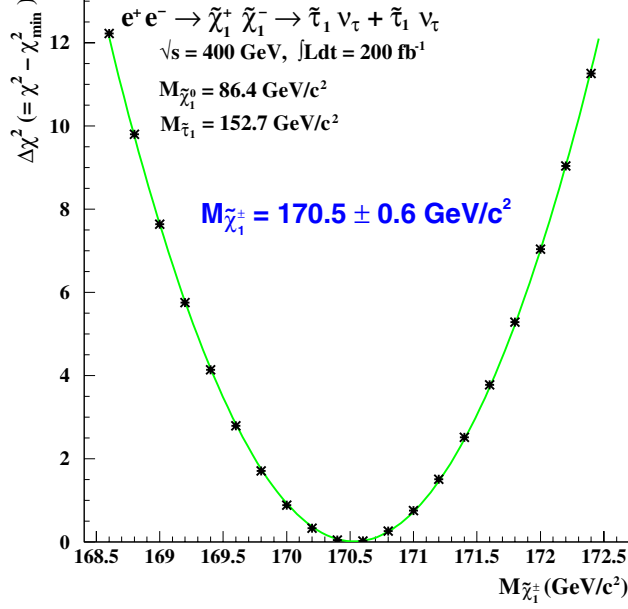


Fig. 2.  $\Delta\chi^2$  of  $\tau$ -jet energy distributions for the reference point

These uncertainties will affect the accuracy in the  $\tilde{\chi}_1^\pm$  mass measurement, because the differences between  $\tilde{\tau}_1^\pm$ ,  $\tilde{\chi}_1^0$ , and  $\tilde{\chi}_1^\pm$  masses determine the shape of  $\tau$ -jet energy distribution. The higher endpoint, in particular, depends on the difference ( $\Delta M$ ) between  $\tilde{\tau}_1^\pm$  and  $\tilde{\chi}_1^\pm$  masses. In order to evaluate the impact of the uncertainties on the  $\tilde{\chi}_1^\pm$  mass determination, we repeat the study for  $M_{\tilde{\chi}_1^\pm} = 171.0 \text{ GeV}/c^2$ , varying  $M_{\tilde{\tau}_1^\pm}$  and  $M_{\tilde{\chi}_1^0}$ . Figure 3 shows a contour plot of  $\Delta\chi^2$  in the  $M_{\tilde{\tau}_1^\pm} - M_{\tilde{\chi}_1^0}$  plane. The center point of each  $\Delta\chi^2$  contour is at  $M_{\tilde{\chi}_1^0} = 84.6 \text{ GeV}/c^2$  and  $M_{\tilde{\tau}_1^\pm} = 151.2 \text{ GeV}/c^2$ . The contours clearly demonstrate a strong positive correlation between  $M_{\tilde{\chi}_1^0}$  and  $M_{\tilde{\tau}_1^\pm}$ , implying that the shape of the  $\tau$ -jet energy distribution is mainly controlled by their difference, as long as the  $\tilde{\chi}_1^\pm$  mass is fixed. It is worth noting that the smallest ellipse, which is the expected  $1\sigma$  bound from the  $\tilde{\tau}_1^\pm$ -pair production study with  $100 \text{ fb}^{-1}$  cited from Ref. [4], has a quite similar correlation and is well contained in the contour corresponding to  $\Delta\chi^2 = 1$ . The aforementioned expected accuracy of  $\pm 0.7 \text{ GeV}/c^2$  for the  $\tilde{\chi}_1^\pm$  mass will hence essentially be unaffected by the inclusion of the uncertainties in the  $\tilde{\chi}_1^0$  and  $\tilde{\tau}_1^\pm$  masses from the lower energy  $\tilde{\tau}_1^\pm$ -pair study.

#### 4.2 Production cross section measurement

The production cross section times branching ratio is experimentally estimated by  $\sigma \cdot \text{Br} = (N_{\text{obs}} - N_{\text{bg}})/(\epsilon_{\text{tot}} \cdot \int \mathcal{L} dt)$ , where  $N_{\text{obs}}$  is the number of observed events,  $N_{\text{bg}}$  the number of expected background events,  $\int \mathcal{L} dt$  the integrated luminosity, and  $\epsilon_{\text{tot}}$  the selection efficiency. It should be noted that  $\epsilon_{\text{tot}}$  weakly depends on  $M_{\tilde{\chi}_1^\pm}$  as shown in Table 2: the efficiency varies by only 0.6% over



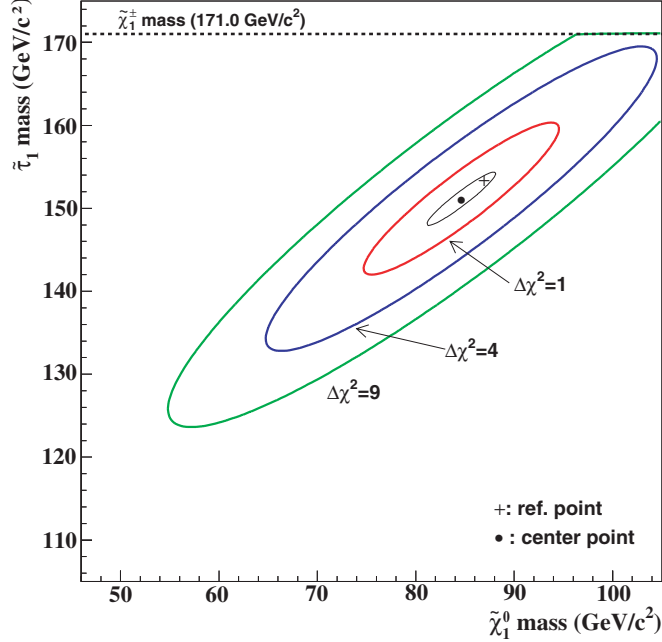


Fig. 3. Contour plot in the  $M_{\tilde{\tau}_1^\pm} - M_{\tilde{\chi}_1^0}$  plane, where  $M_{\tilde{\chi}_1^\pm}$  can be measured to an accuracy of  $\pm 0.7 \text{ GeV}/c^2$  ( $\Delta\chi^2 = 1$ ),  $\pm 1.4 \text{ GeV}/c^2$  ( $\Delta\chi^2 = 4$ ), and  $\pm 2.1 \text{ GeV}/c^2$  ( $\Delta\chi^2 = 9$ ). The smallest ellipse is the expected  $1\sigma$  bound for the  $\tilde{\chi}_1^0$  and  $\tilde{\tau}_1^\pm$  mass fit with  $100 \text{ fb}^{-1}$  cited from Ref. [4].

the mass range of  $\pm 20 \text{ GeV}/c^2$  from  $M_{\tilde{\chi}_1^\pm}^{\text{ref}}$ . This implies the possibility of extracting the cross section times branching fraction ( $\sigma \cdot \text{Br} = 322 \pm 6 \text{ fb}$ ) independently of the input  $\tilde{\chi}_1^\pm$  mass, provided that  $\int \mathcal{L} dt = 200 \pm 2 \text{ fb}^{-1}$  (the luminosity is assumed to be measured with an uncertainty of 1% [4]),  $N_{\text{obs}} - N_{\text{bg}} = 10175$  events (the background contribution is fully estimated), and  $\epsilon_{\text{tot}} = 0.158 \pm 0.002$  (the uncertainty includes the weak dependence of  $\epsilon_{\text{tot}}$  on  $M_{\tilde{\chi}_1^\pm}$ ). This indicates that we can determine the production cross section times branching fraction to an accuracy of 2% even without any precise  $M_{\tilde{\chi}_1^\pm}$  study.

## 5 Summary

At large  $\tan\beta$  values, the  $\tilde{\tau}_1^\pm$  mass might be lighter than the  $\tilde{\chi}_1^\pm$  mass within the MSSM framework. In this case, the  $\tilde{\chi}_1^\pm \rightarrow \tilde{\tau}_1^\pm \nu_\tau$  decay will be dominant and that will be followed by  $\tilde{\tau}_1^\pm \rightarrow \tau^\pm \tilde{\chi}_1^0$ . We have thus studied the final state consisting of  $\tau\tau$  + large missing energy as a possible signature of the chargino pair production at a future  $e^+e^-$  linear collider.

We proposed to use the  $\tau$ -jet energy distribution to measure the  $\tilde{\chi}_1^\pm$  mass in the large  $\tan\beta$  scenario. Since this scenario leads  $\tilde{\chi}_1^0$  and  $\tilde{\tau}_1^\pm$  masses to be lighter

than  $\tilde{\chi}_1^\pm$  mass and opens the  $\tilde{\tau}_1^\pm$  pair production mode with lower energy of  $\tilde{\chi}_1^\pm$  pair production, the  $\tilde{\chi}_1^0$  and  $\tilde{\tau}_1^\pm$  masses are likely to be determined in the lower  $\tilde{\chi}_1^\pm$  production threshold energy operation of the collider. The measurements of 171 GeV/ $c^2$  chargino could then be made with an accuracy better than 1 GeV/ $c^2$ , provided that the  $\tilde{\chi}_1^0$  and  $\tilde{\tau}_1^\pm$  masses will have been determined through a  $\tilde{\tau}_1^\pm$ -pair production study with 100 fb $^{-1}$ .

Since the event selection efficiency does not significantly depend on the  $\tilde{\chi}_1^\pm$  mass, the uncertainty in the production cross section shall be dominated by uncertainties in the selection efficiency and the luminosity measurement. We expect to determine the cross section to an accuracy of 2% at the reference point despite the cascade decay mode.

## Acknowledgements

The authors would like to thank R. Arnowitt for carefully reading the manuscript. Y.K. is supported by the Grant for Kinki University, while K.F. is supported in part by Japan-Europe (UK) Research Cooperation Program and JSPS-CAS Scientific Cooperation Program under the Core University System, T.K. and V.K. by U.S. Department of Energy grant DE-FG02-95ER40917, and M.M.N. by the Grant-in-Aid for Science Research, Ministry of Education, Science and Culture, Japan (No.14540260 and No.14046210), respectively.

## References

- [1] H.P. Nilles, *Phys. Rep.* **110** (1984) 1; H.E. Haber and G.L. Kane, *Phys. Rep.* **117** (1985) 75.
- [2] T. Tsukamoto, K. Fujii, H. Murayama, M. Yamaguchi, and Y. Okada, *Phys. Rev. D* **51** (1995) 3153; J. Feng, M. Peskin, H. Murayama, and X. Tata, *Phys. Rev. D* **52** (1995) 1418; S.Y. Choi, M. Guchait, J. Kalinowski, and P.M. Zerwas, *Phys. Lett. B* **479** (2000) 235; J.A. Aguilar-Saavedra, et al., *TESLA Technical Design Report, Part III: Physics at an  $e^+e^-$  Linear Collider*, DESY 2001-11(2001); T. Abe et al.(American Linear Collider working group), *Linear Collider physics resource book for Snowmass 2001, Part2: Higgs and Supersymmetry studies*, SLAC-R-570(2001).
- [3] M. Nojiri, K. Fujii, and T. Tsukamoto, *Prog. Theor. Phys. Suppl.* **123** (1996) 203.
- [4] M. Nojiri, K. Fujii, and T. Tsukamoto, *Phys. Rev. D* **54** (1996) 6756.
- [5] D. N Spergel, et al. (WMAP Collaboration), *Astrophys. J. Suppl.* **148** (2003) 175.

- [6] R. Arnowitt, B. Dutta, T. Kamon, and V. Khotilovich, hep-ph/041102;
- [7] H. Baer, T. Krupovnickas, and X. Tata, *JHEP* **0406** (2004) 61.
- [8] P. Bambade, M. Berggren, F. Richard, and Z. Zhang, hep-ph/0406010.
- [9] H. Murayama, I. Watanabe, and K. Hagiwara, KEK Report No.91-11 (1992).
- [10] S. Kawabata, *Comput. Phys. Comm.* **41** (1986) 127.
- [11] S. Jadach and J. H. Kühn, *Comput. Phys. Comm.* **64** (1991) 275; M. Jeżabek, Z. Was, S. Jadach, and J. H. Kühn, *Comput. Phys. Comm.* **70** (1992) 69; M. Jeżabek, Z. Was, S. Jadach, and J. H. Kühn, *Comput. Phys. Comm.* **76** (1993) 361. We use version 2.3
- [12] K. Fujii, T. Matsui, and Y. Sumino, *Phys. Rev. D* **50** (1994) 4341.
- [13] JLC Group, *JLC I*, KEK Report No.92-16 (1992).
- [14] JADE Collaboration, W. Bartel et al., *Z. Phys. C* **33** (1986) 23; JADE Collaboration, S. Bethke et al., *Phys. Lett. B* **213** (1988) 235.
- [15] CERN Program Library Entry D506 (1998).